Journal of Pathology
J Pathol 2015; **235:** 65–78
Published online 6 November 2014 in Wiley Online Library (wileyonlinelibrary.com) DOI: 10.1002/path.4423

ORIGINAL PAPER

Macrophage-specific NOX2 contributes to the development of lung emphysema through modulation of SIRT1/MMP-9 pathways

Candice Trocme,[1] Christine Deffert,[2,3] Julien Cachat,[2] Yves Donati,[2,4] Christelle Tissot,[2] Sylvie Papacatzis,[1] Vincent Braunersreuther,[5] Jean-Claude Pache,[5] Karl-Heinz Krause,[2] Rikard Holmdahl,[6] Constance Barazzone-Argiroffo[2,4] and Stéphanie Carnesecchi[2,4]*

[1] *Laboratory of Protein and Enzyme Biochemistry, University Hospital, Grenoble, France*
[2] *Department of Pathology and Immunology, Medical School, University of Geneva, Switzerland*
[3] *Department of Medicine Genetic and Laboratory (DMGL), University Hospital, Geneva, Switzerland*
[4] *Department of Pediatrics, University Hospital, Geneva, Switzerland*
[5] *Department of Clinical Pathology, Medical School, University of Geneva, Switzerland*
[6] *Division of Medical Inflammation Research, Department of Medical Biochemistry and Biophysics (MBB), Karolinska Institutet, Sweden*

**Correspondence to: Stephanie Carnesecchi, Departments of Pathology–Immunology and Pediatrics, Centre Médical Universitaire, 1 Rue Michel Servet, 1211 Geneva 4, Switzerland. E-mail: Stephanie.Carnesecchi@unige.ch*

Abstract

Reactive oxygen species (ROS) participate in the pathogenesis of emphysema. Among ROS-producing enzymes, NOX NADPH oxidases are thought to be responsible for tissue injury associated with several lung pathologies. To determine whether NOX2 and/or NOX1 participate in the development of emphysema, their expression patterns were first studied by immunohistochemistry in the lungs of emphysematous patients. Subsequently, we investigated their contribution to elastase-induced emphysema using NOX2- and NOX1-deficient mice. In human lung, NOX2 was mainly detected in macrophages of control and emphysematous lungs, while NOX1 was expressed in alveolar epithelium and bronchial cells. We observed an elevated number of NOX2-positive cells in human emphysematous lungs, as well as increased *NOX2* and *NOX1* mRNA expression in mouse lungs following elastase exposure. Elastase-induced alveolar airspace enlargement and elastin degradation were prevented in NOX2-deficient mice, but not in NOX1-deficient mice. This protection was independent of inflammation and correlated with reduced ROS production. Concomitantly, an elevation of sirtuin 1 (SIRT1) level and a decrease of matrix metalloproteinase-9 (MMP-9) expression and activity were observed in alveolar macrophages and neutrophils. We addressed the specific role of macrophage-restricted functional NOX2 in elastase-induced lung emphysema using *Ncf1* mutant mice and *Ncf1* macrophage rescue mice (*Ncf1* mutant mice with transgenic expression of Ncf1 only in CD68-positive mononuclear phagocytes; the MN mouse). Compared to WT mice, the lack of functional NOX2 led to decreased elastase-induced ROS production and protected against emphysema. In contrast, ROS production was restored specifically in macrophages from *Ncf1* rescue mice and contributes to emphysema. Taken together, our results demonstrate that NOX2 is involved in the pathogenesis of human emphysema and macrophage-specific NOX2 participates in elastase-induced emphysema through the involvement of SIRT1/MMP-9 pathways in mice.

Keywords: ROS; NOX2; MMP-9; SIRT1; emphysema; macrophages

Received 14 March 2014; Revised 5 August 2014; Accepted 5 August 2014

No conflicts of interest were declared.

Introduction

Pollution and tobacco smoke exposure are associated with the pathogenesis of chronic obstructive pulmonary disease (COPD). Emphysema, which is part of COPD, is clinically characterized by small airway inflammation and airspace enlargement due to lung alveolar destruction [1]. This disease affects millions of individuals and its progression cannot be stopped with available treatments. Indeed, the molecular mechanisms that underlie its pathogenesis are not clearly defined. Thus, while oxidative stress is known to participate in the pathogenesis of emphysema [2–6], it is still unclear whether lung destruction is mainly due to oxidant produced by inflammatory cells and/or is aggravated by those produced by damaged alveolar cells.

Among ROS-producer enzymes, the NADPH oxidase family, a complex including a catalytic subunit called NOX associated with regulatory subunits [7,8], is thought to be responsible for lung damage found in several lung pathologies. NOX2, which is highly expressed in inflammatory cells, plays an essential role in non-specific host defence against pathogens and is defective in the genetic disorder chronic granulomatous disease [9]. The other NOX isoforms, named NOX1–4 and DUOX1/2, have been described in several lung

cell types and are associated with lung pathological situations [10–19]. Some studies indicate that NOX enzymes contribute to the pathogenesis of COPD. Indeed, cigarette smoke (CS) induces expression of NOXO1, a regulatory subunit of NOX1, the isoform preferentially expressed in lung epithelial cells [20]. In addition, deficiency of NOX2 or Ncf1/p47^{phox} (a critical regulatory subunit of NOX2) has been reported to prevent lung inflammation in mice exposed to CS [21], and NOX3 was correlated to age-related emphysema in mice [22]. However, other studies demonstrated that NOX2 deficiency contributes to age-related emphysema in mice and sensitizes mice to CS [22,23]. Thus, the contributions of NOX1 and NOX2 in the pathogenesis of lung emphysema, as well as the characterization of cell-type-specific molecular and cellular mechanisms, need to be addressed. In addition, the expression patterns of NOX1 and NOX2 as well as their specific cell type localizations have never been described in the lungs of emphysematous patients.

Materials and methods

Control and emphysematous patients

Emphysematous and control lung biopsies ($n = 10$ each) were obtained by thoracotomy in accordance with an approved protocol by the Institutional Ethical Committee of Geneva (Authorization No 11-087R NAC 11-027R).

Human lung immunostaining

Paraffin-embedded sections of lung fixed in 4% PFA were stained with anti-NOX1 (1 : 500 [24,25]) or anti-NOX2 (1 : 2000; LS Bio 48, Seattle, WA, USA) or anti-CD68 (1 : 100; DAKO, Carpinteria, CA, USA) or anti-pro-surfactant C (1 : 1000; Chemicon, Darmstadt, Germany), followed by incubation with horseradish peroxidase anti-rabbit or mouse (Envision System, DAKO) with diaminobenzidine (DAB; DAKO). Sections were counterstained with Mayer's hemalum. Negative controls were obtained by incubating the sections with rabbit IgG or mouse IgG1 isotype control (1 : 1000, 1 : 10, respectively; Vector Laboratories, Servion, Switzerland). Lung slides were scanned (Mirax, Zeiss) and quantification of positive staining was performed on scanned images with Metamorph analysis software (one slide per subject, 5–6 subjects per group).

Animals and experimental design

NOX1-, NOX4-, NOX2-deficient, and wild-type (WT) mice were inbred on a C57BL/6 J background [12,26,27], and *Ncf1* mutants and *Ncf1* macrophage rescue transgenic mice (MN) were on a B10.Q background as described previously [28]. Mice aged 8–12 weeks and NOX2-deficient mice at the age of 12 months were maintained in specific pathogen-free (SPF) conditions. All animal experiments were approved by the Institutional Ethical Committee of Animal Care in Geneva and Cantonal Veterinary Office (Authorization: GE/16/14). Porcine pancreatic elastase (3 U/25 g; Elastin Products, Owensville, MO, USA) or vehicle (saline) was instilled into the tracheae of WT and genetically modified mice under anaesthesia as previously described [12]. Mice were killed at days 2 and 21, and lungs were processed for subsequent analysis.

Administration of sirtinol

Sirtinol (2 mg/kg; Calbiochem, San Diego, CA, USA) was administered by intraperitoneal injection [29] 1 h prior to elastase instillation and every 2 days for 21 days to WT and NOX2-deficient mice.

Mouse lung histology and morphometry

Lung was fixed by intratracheal instillation of 4% PFA at a pressure of 25 cm H_2O and embedded in paraffin. Sections (3 µm) were stained with haematoxylin and eosin (H&E) or with Victoria Blue. Stained lung sections were scanned using a Slide Scanner (Mirax, Zeiss) and the mean linear intercept (L_m) of the airspace was measured using Image J software on ten randomly selected fields at a magnification of × 100 in a blind manner.

Western blot

Lung protein extracts were prepared as previously described [10]. Proteins blotted on nitrocellulose membrane were incubated with anti-SIRT1 (1 : 1000; Cell Signaling, Schaffhausen, Switzerland) or anti-actin (1 : 1000; Sigma, Buchs, Switzerland), followed by incubation with peroxidase-conjugated anti-mouse or rabbit. Proteins were detected with ECL reagents (Amersham Pharmacia Biotech, Basel, Switzerland). Densitometric evaluation was performed using Quantity One software (Bio-Rad Laboratories, Hercules, CA, USA).

Bronchoalveolar lavage, protein level, cell count, and cytokine measurement

Bronchoalveolar lavage (BAL) was collected as described previously [10]. Total cell count was determined with a Neubauer chamber and protein concentration was measured [10]. BAL cell distribution was quantified in Cytospin preparations (Perbio Science, Lausanne, Switzerland) after staining with Diff-Quik dye (Dade Behring, Courbevoie, France).

The amount of IL-6 was measured in BAL and CXCL1 and CXCL2 in lung homogenates [30] by enzyme-linked immunosorbent assay ELISA kits (R&D Systems, Abingdon, UK).

Detection of reactive oxygen species

To detect cell types generating ROS, frozen lung sections (20 µm) were double-immunostained with

dihydroethidium (DHE, 5 μM) and anti-IBA1 (1/500; WAKO, Neuss, Germany) or with DHE and anti-MPO (myeloperoxidase; 1/1000; DAKO) or with DHE and anti-von Willebrand factor (vWF; 1/250; DAKO). Images were captured with a confocal microscope (LSM 510 Meta, Zeiss) and analysed using Metamorph software.

Detection of DNA oxidation

After blocking, fixed and permeabilized frozen lung sections (6 μm) were stained with an anti-8-hydroxy-2′-deoxyguanosine (8-OHdG) antibody (1/30; Oxis, Beverly Hills, CA, USA) followed by a goat anti-mouse dye light conjugated (1/200; Molecular Probes, Lucerne, Switzerland). Nuclei were stained with 4,6-diamidino-2-phenylindole (DAPI) (1 : 200; Roche Diagnostics, Basel, Switzerland). Slides were mounted with fluorsave (VWR) and analysed by confocal microscopy (LSM 510 Meta, Zeiss). Quantification was performed by measuring the number of 8-OHdG-positive cells of all nuclei counted ($n > 100$) in lung sections from three different mice per group.

TUNEL assay

TUNEL detection in BAL was performed as described by the manufacturer (TUNEL assay fluorescent kit, Roche). Slides were mounted with fluorsave (VWR) and analysed by confocal microscopy. Quantification of positive staining was performed using Metamorph analysis software (ten images per mouse, three mice per group out of three independent experiments).

Real-time PCR

RNA was extracted with the RNeasy Protect mini kit (Qiagen, Valencia, CA, USA) and reverse-transcribed using the superscript reverse transcriptase (Superscript Choice, Invitrogen, Switzerland). A total of 0.5 μg of sample was used as a template for the real-time PCR. Primer sequences are described in the Supplementary materials and methods.

Matrix metalloproteinases and TIMP-1 measurement

Lungs were mechanically homogenized in RIPA lysis buffer [31]. Matrix metalloproteinases MMP-9 and MMP-2 were evaluated by zymography in lung homogenates and BAL as described previously [32]. MMP levels were calculated by reference to the scanning values obtained from known amounts of purified MMP-9 and MMP-2. MMP-9 and MMP-2 levels were expressed in pg per μg of protein for lung homogenates and in ng per μl for BAL.

Tissue inhibitor of metalloproteinase 1 (TIMP-1) levels were measured in lung homogenates and BAL using a Mouse TIMP-1 Quantikine ELISA Kit according to the manufacturer's instructions (R&D Systems, Switzerland). Results were expressed in pmol of TIMP-1 per μg of protein.

SIRT1 immunostaining

Frozen lung sections (6 μm) were fixed with 4% PFA and permeabilized with 0.1% Tx-100 in 0.1% sodium citrate. After blocking, sections were incubated with anti-SIRT1 (1 : 200; Millipore) and anti-IBA1 or anti-MPO, followed by a goat anti-rabbit Texas Red conjugated antibody (1 : 250; Molecular Probes). The nuclei were stained with DAPI (1 : 200; Roche Diagnostics). Slides were mounted with fluorsave (VWR) and analysed by confocal microscopy (LSM 510 Meta, Zeiss).

Statistical analysis

Results are expressed as mean ± SEM and ± SD as indicated and were analysed by parametric (*t*-tests) and non-parametric (Mann–Whitney) tests. In the case of multiple comparisons, a two-way ANOVA test was used and adjusted with Bonferroni's correction. Significance levels were set at $p < 0.05$.

Results

NOX2 is expressed in lung macrophages of emphysematous lungs, whereas NOX1 is detected in alveolar epithelial cells

We first studied the expression of NOX1 and NOX2 in lung sections of control and emphysematous patients by immunohistochemistry (Figure 1). In control lungs, NOX1 was only detected in alveolar endothelial cells (data not shown) and macrophages (Figure 1A, asterisk), whereas epithelial cells (Figure 1A, arrow) were negative for NOX1, as previously demonstrated [33]. In emphysematous lungs, NOX1 was highly expressed in bronchial (Figure 1A, ampersand) and type II epithelial cells (Figure 1A, arrows), whereas NOX2 was mainly detected in alveolar (Figure 1B, arrow) and interstitial macrophages (Figure 1B, arrowhead) in both control and emphysematous lungs.

The cell-type-specific localizations were confirmed by serial immunostaining of emphysematous lung sections with an anti-NOX1 antibody and a specific marker for type II epithelial cells [anti-pro-surfactant C (SPC)], and with an anti-NOX2 antibody and a pan-macrophage marker (anti-CD68). We detected NOX1 in type II epithelial cells (Figure 1C, arrow) and NOX2 was found to be positive for CD68-positive alveolar and interstitial macrophages (arrow and arrowhead, respectively).

The number of NOX2-positive cells was then quantified in lung sections of both control and emphysematous patients. A marked increase of NOX2-positive cells was observed in emphysematous versus control lungs (28.11 ± 10.34 versus 60.62 ± 34.47, $^{*}p = 0.017$).

Thus, NOX1 is preferentially expressed in alveolar and bronchial epithelium of emphysematous lungs, whereas NOX2 is mainly found in inflammatory cells, particularly macrophages.

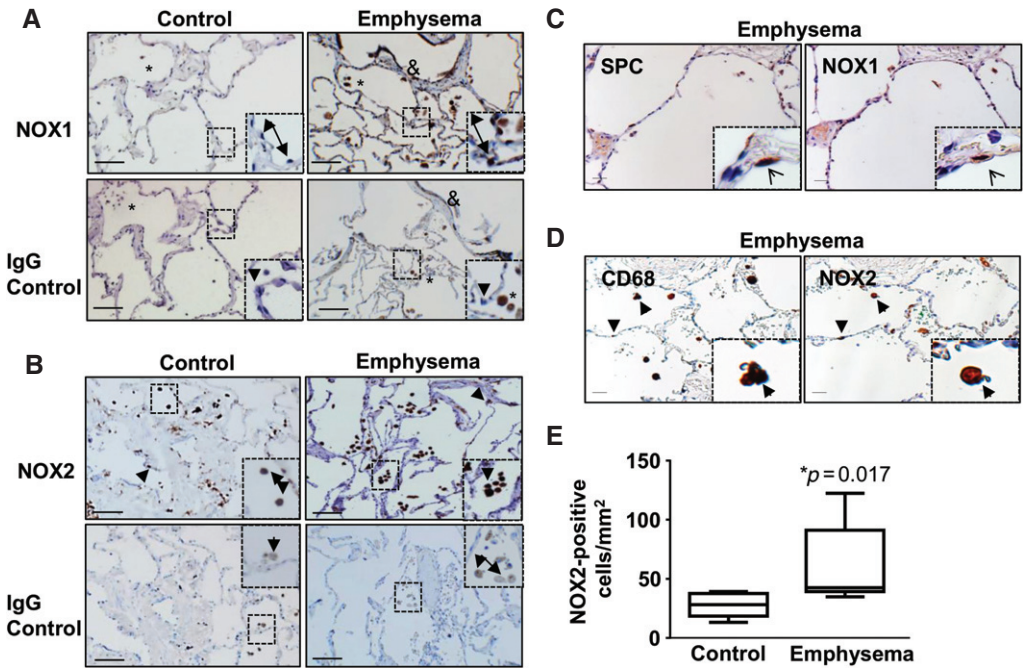

Figure 1. NOX2 is expressed in alveolar macrophages and NOX1 in lung epithelial cells of emphysematous patients. Sections of emphysematous and control lung were stained with specific anti-NOX1 (A) and anti-NOX2 antibodies (B). Negative controls were obtained by incubating sections with specific isotype controls (lower panels). Boxes represent magnified regions of normal or emphysematous parenchyma. Arrows indicate either cells stained with anti-NOX1 antibody (A) or NOX2-positive cells (B). The asterisk indicates NOX1-positive macrophages and the ampersand NOX1-positive bronchial epithelium. (C) Serial lung sections of emphysematous patients were stained with an anti-NOX1 antibody and pro-surfactant C (SPC), a specific marker of type II epithelial cells. Epithelial type II cells are positive for NOX1 (arrow). (D) Serial sections of emphysematous lung were stained with an anti-NOX2 antibody and anti-CD68 antibody. Note the expression of NOX2 in CD68-positive macrophages (arrow). Scale bars = 500 μm. (E) Quantification of the number of NOX2-positive cells in airspaces and alveolar wall tissue of control and emphysematous patients per mm^2 of surface area. The number of NOX2-positive cells, principally macrophages, is significantly increased in emphysematous patients versus controls ($n = 5–6$ subjects per group; Mann–Whitney; $^*p = 0.017$).

NOX2 deficiency but not NOX1 protected against elastase-induced lung emphysema

To establish the role of NOX2, NOX1, and NOX4 in the development of emphysema, we intratracheally instilled wild-type C57Bl/6 mice and NOX1-, NOX4- and NOX2-deficient mice with elastase or saline alone.

We first measured the expression of NOX1, NOX2, NOX3, NOX4, and DUOX2 in the lungs of WT mice treated with saline or elastase for 2 and 21 days, using quantitative PCR. The levels of *NOX1* and *NOX2* mRNA increased in elastase-treated mice at day 2 compared with controls and returned to baseline at day 21 (Figure 2A). It should be noted that gene expression of other NOX members was not modulated by elastase exposure (Figure 2A).

We then compared the impact of elastase on the development of emphysema in WT and deficient mice, using morphometric analysis. WT, NOX1-, and NOX4-deficient mice presented massive alveolar destruction, as shown by measurement of the mean linear intercept (Figures 2B and 2C) and histochemical analysis of Victoria Blue staining (elastin staining, Figures 2D and 2E), whereas few emphysematous lesions were observed in NOX2-deficient mice (Figures 2B–2D). It should be noted that no compensatory regulation of NOXs (NOX1, NOX3, NOX4, and DUOX2) was detected in lungs between WT and NOX2-deficient mice exposed to elastase (Supplementary Figure 1).

Thus, NOX2-deficient, but not NOX1- and NOX4-deficient, mice are protected against emphysema in response to elastase.

Elastase-induced ROS production is dependent on NOX2 specifically in inflammatory cells

To determine the contribution of NOX2 and NOX1 in elastase-induced ROS production and DNA oxidation, DHE and 8OHDG staining was performed on frozen lung sections. ROS production (Figures 3A and 3C) and DNA oxidation (Figures 3B and 3D) were increased in WT and NOX1-deficient mice following elastase exposure, which was blunted in NOX2-deficient mice.

To identify the cell types generating ROS, we performed co-staining with DHE and specific markers for macrophages (IBA-1), neutrophils (myeloperoxidase, MPO), and endothelial cells (von Willebrand factor, vWF). Macrophages (Figure 3E, arrow) and neutrophils (Figure 3E, arrow), but not endothelial cells (Figure 3E, arrow), were positive for DHE staining in WT mice after elastase stimulation. By contrast, elastase-induced ROS production was not detectable in macrophages and neutrophils from NOX2-deficient mice (Figure 3E, arrow).

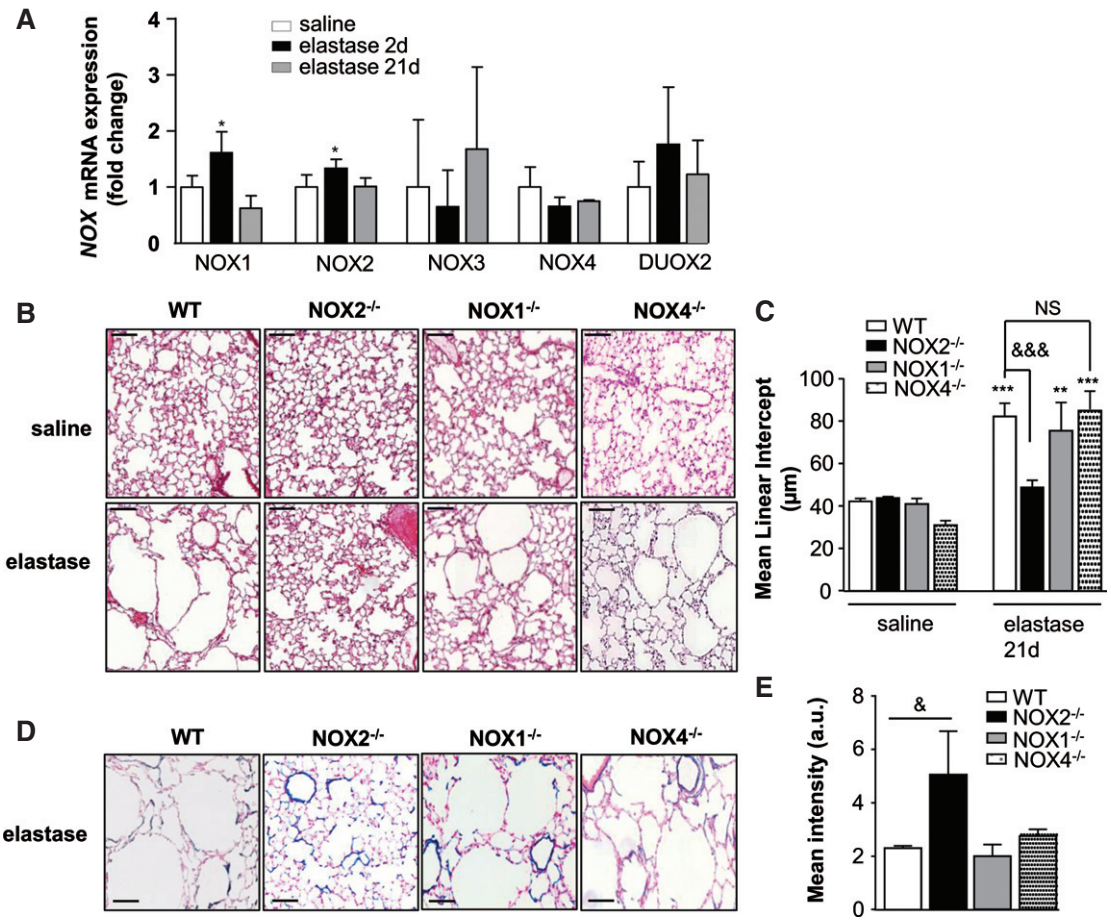

Figure 2. NOX2-deficient mice are protected against elastase-induced lung emphysema. (A) Expression of *NOX1*, *NOX2*, *NOX3*, *NOX4*, and *DUOX2* mRNA in lungs of WT mice treated with saline or elastase at days 2 and 21. Note the increased *NOX1* and *NOX2* mRNA levels at day 2 of elastase stimulation. (B) Lung histology of WT and NOX1-, NOX2-, and NOX4-deficient mice exposed to elastase or saline at day 21. Typical enlargement of the alveolar spaces was observed in elastase-exposed WT, NOX4-, and NOX1-deficient mice but not in NOX2-deficient mice. (C) Quantification of alveolar diameter expressed as mean linear intercept (L_m, µm). (D) Blue Victoria staining for elastin was performed in lungs of WT and NOX2-, NOX4-, and NOX1-deficient mice following elastase exposure. (E) Quantification of Blue Victoria staining expressed as mean intensity (arbitrary units, a.u.). NOX2-deficient mice present a smaller alveolar airspace enlargement and amount of elastin in the elastic fibres compared with elastase-exposed WT, NOX4-, and NOX1-deficient mice. Scale bars = 100 µm. Data ± SEM; $n = 3–8$ mice per group; p = NS, $^{*}p < 0.05$, $^{**}p < 0.01$, $^{***}p < 0.001$ saline versus elastase; $^{\&}p < 0.05$, $^{\&\&\&}p < 0.001$ WT versus NOX2$^{-/-}$ upon elastase exposure.

It should be noted that elastase also induces ROS production in epithelial cells (Figure 3E, arrowhead, upper panels), which is abolished in NOX2-deficient mice. Thus, production of ROS in lung macrophages and neutrophils following elastase exposure depends on NOX2.

NOX2-deficient mice are protected against emphysema despite sustained inflammation

As lung inflammation is a key factor in elastase-induced lung emphysema [1], we determined whether the protection afforded by NOX2 deficiency is linked to modulation of inflammation. BAL cell count (Figures 4A–4C) and levels of selected pro-inflammatory cytokine and neutrophil-chemoattractant chemokines (CXCL1, CXCL2) (Supplementary Figures 2A–2C) were measured.

Instillation of elastase led to an increase in BAL cell count in all mouse strains tested (WT, NOX1-, and NOX2-deficient mice) but the NOX2-deficient mice had a significantly higher response at day 2. In all groups, the response returned to baseline after 3 weeks (Figure 4A). The number of BAL macrophages was increased at both 2 days and 21 days after elastase instillation but was not significantly different between WT, NOX1-, and NOX2-deficient mice (Figure 4B). Interestingly, NOX2-deficient mice showed an increased number of neutrophils compared with WT and NOX1-deficient mice exposed to elastase at day 2 (Figure 4C), without any modification of the levels of pro-inflammatory cytokine (IL-6) and neutrophil-chemoattractant chemokines (CXCL1 and CXCL2) (Supplementary Figures 2A–2C). Nevertheless, an accumulation of apoptotic neutrophils was observed in BAL of NOX2-deficient mice under elastase exposure (TUNEL staining, Figures 4D–4F).

Taken together, this suggests that absence of NOX2 in alveolar macrophages and neutrophils prevents the development of emphysema, despite a sustained inflammatory response.

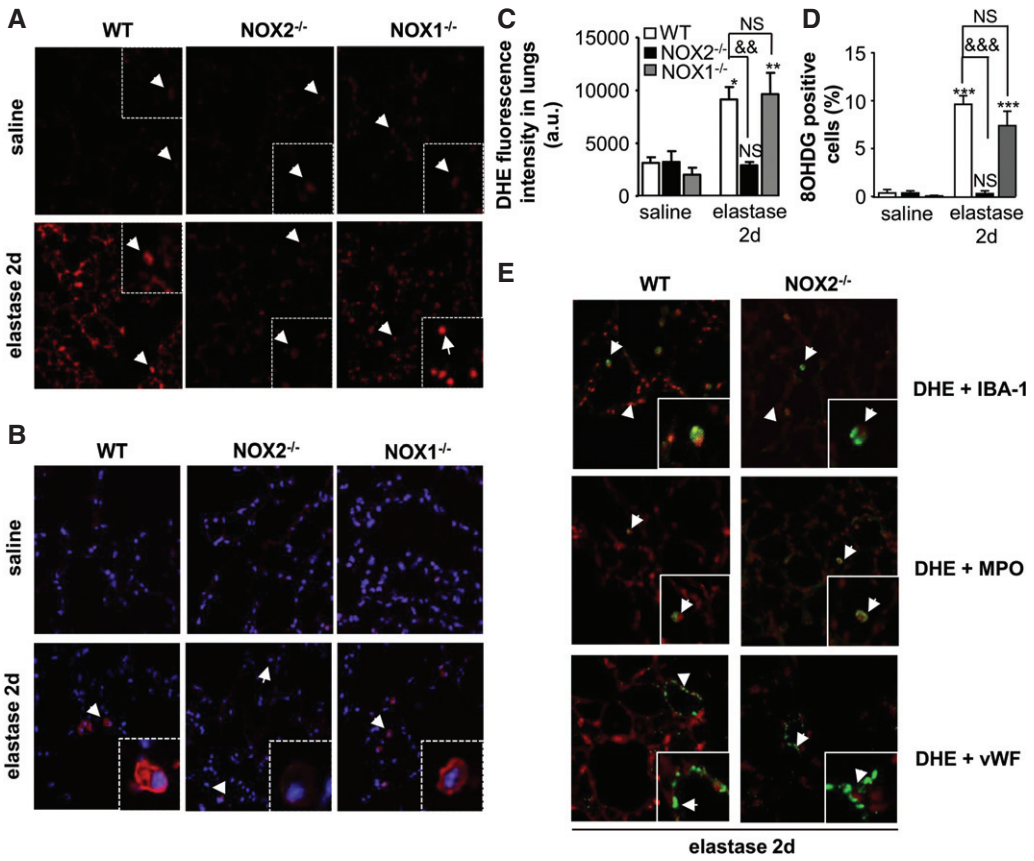

Figure 3. Elastase-induced ROS production in lungs is dependent on NOX2. (A) Representative lung sections from saline and elastase-exposed WT, NOX1-, and NOX2-deficient mice loaded with dihydroethidium (red) and (B) stained with an anti-8OHDG antibody (red). Arrows indicate alveolar macrophages positive for DHE staining, according to their localization. Original magnification: × 40. (C) Quantification of reactive oxygen species (ROS) generation in lungs expressed as DHE fluorescence intensity (arbitrary units, a.u.). (D) Quantification of DNA oxidation by counting 8OHDG-positive cells (red) relative to the total number of nuclei (blue). Data ± SEM; $n = 3-4$ mice per group; p = NS, $^{**}p < 0.01$, $^{***}p < 0.001$ saline versus elastase; $^{\&\&}p < 0.01$, $^{\&\&\&}p < 0.001$ WT versus NOX2$^{-/-}$ upon elastase exposure. (E) Representative merged images of lungs loaded with DHE (red) and specific markers for macrophages (IBA-1, green) or for neutrophils (myeloperoxidase, MPO, green) or for endothelial cells (von Willebrand factor, vWF, green). Note that cells are positive for DHE and macrophages and neutrophil-specific markers but not for the endothelial-specific marker (arrow). We also observed that epithelial cells (arrowhead) are positive for DHE and that DHE fluorescence in these cells is abolished in NOX2-deficient mice.

Deficiency of NOX2 reduces elastase-induced MMP-9 expression and activity

Increased expression of MMP-9 contributes to the pathogenesis of emphysema [34,35], and its expression and activity are known to be regulated by oxidative stress [36,37]. In this context, we first analysed *MMP-2*, *MMP-9*, and *MMP-12* mRNA in lung tissues of WT and NOX2-deficient mice (Figure 5). Elastase-treated WT mice showed an increase of MMP-9, but not of MMP-2 or MMP12, after 2 days, which was not seen in NOX2-deficient mice (Figures 5A–5C).

We therefore quantified the levels of MMP-9 and MMP-2 as well as TIMP-1 in lungs and BAL by zymography (Figure 6 and Supplementary Figure 3). The MMP-9 protein level (pro- + active-MMP-9 forms) was increased in the lungs and BAL of WT mice after elastase stimulation, which was significantly reduced by the deficiency of NOX2 (Figures 6A and 6C–6E). No modification of TIMP-1 and MMP-2 protein levels was observed between WT and NOX2-deficient mice following elastase stimulation (Figures 6B, 6C, and 6F and Supplementary Figures 3A and 3B). In addition, elastase led to increased BAL MMP-9 activity (active form, Figures 6C and 6D) in WT mice, which was diminished in NOX2-deficient mice.

Taken together, these results demonstrate that following elastase stimulation, NOX2 contributes to the increased MMP-9 expression and activity without modifying TIMP-1 in inflammatory cells.

NOX2 contributes to elastase-induced emphysema through negative regulation of SIRT1 in both macrophages and neutrophils

Sirtuin 1 (SIRT1), a redox-sensitive protein, is a negative regulator of MMP-9 expression [38] and protects against emphysema [29]. To further understand the mechanisms underlying NOX2-induced MMP-9 expression in elastase-induced emphysema, we investigated the effect of NOX2 deficiency on SIRT1 expression in lung homogenates by western blot and immunostaining (Figures 7A–7C). Elastase reduced the level of SIRT1 in the lungs of WT mice, but not in NOX2-deficient

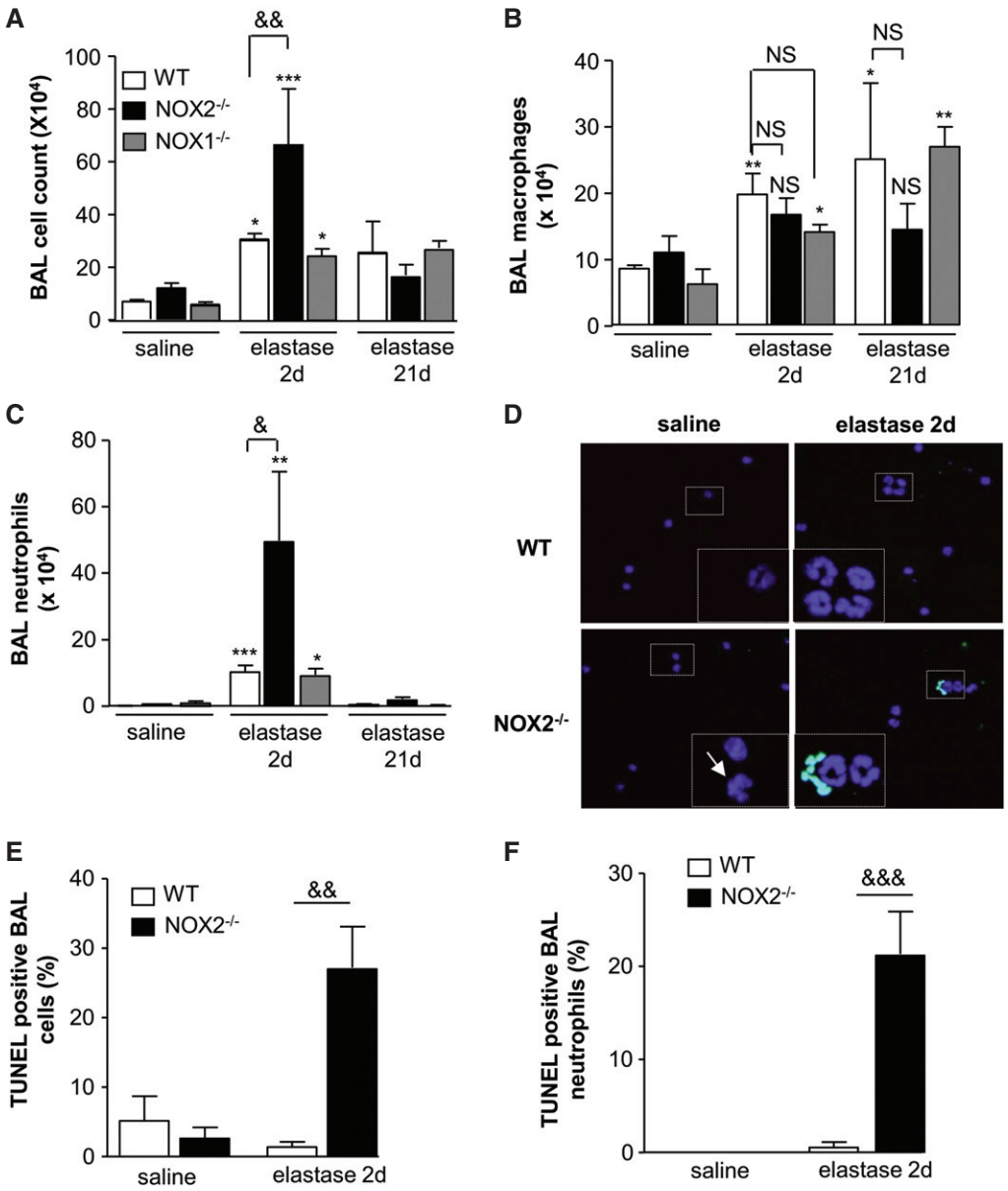

Figure 4. NOX2 does not contribute to elastase-induce emphysema through inflammatory processes. (A) Total cell count in bronchoalveolar lavage (BAL) of WT, NOX1-, and NOX2-deficient mice exposed to saline or elastase at days 2 and 21. Saline-exposed: $n = 13$ WT, $n = 15$ NOX2-deficient, $n = 7$ NOX1-deficient; elastase-exposed at day 2: $n = 11$ WT, $n = 9$ NOX2-deficient, $n = 3$ NOX1-deficient; elastase-exposed at day 21: $n = 3$ per group. Macrophages (B) and neutrophils (C) were counted on cytospin preparations. Data ± SEM; saline-exposed: $n = 9$ WT, $n = 12$ NOX2-deficient, $n = 3$ NOX1-deficient mice; elastase-exposed at day 2: $n = 11$ WT, $n = 9$ NOX2-deficient, $n = 3$ NOX1-deficient mice; elastase-exposed at day 21: $n = 3$ mice per group; p = NS, $^{*}p < 0.05$, $^{**}p < 0.01$, $^{***}p < 0.001$ saline versus elastase; $^{\&\&}p < 0.01$, $^{\&\&\&}p < 0.001$ WT versus NOX2$^{-/-}$. (D) Representative merged images of cytospin stained with TUNEL (green) and DAPI (blue). TUNEL-positive cells appear in light blue (arrow). (E) TUNEL-positive BAL cell number expressed as percent of all nuclei counted on cytospin. (F) TUNEL-positive BAL neutrophil number expressed as per cent of all nuclei counted on cytospin. Neutrophils were counted according to their nuclear morphology. Data ± SEM; $n = 3$ mice per group; p = NS, $^{*}p < 0.05$, **p < 0.01, $^{***}p < 0.001$ saline versus elastase; $^{\&\&}p < 0.01$, $^{\&\&\&}p < 0.001$ WT versus NOX2$^{-/-}$.

mice (Figures 7A–7C). It should be noted that this effect persisted until 21 days following elastase instillation in NOX2-deficient mice (Supplementary Figure 4).

To identify SIRT1-positive cell types, we stained lung sections from WT and NOX2-deficient mice exposed to elastase with an anti-SIRT1 antibody and specific markers for macrophages (IBA-1) and neutrophils (MPO) (Figures 7D and 7E). Elastase-induced SIRT1 reduction was rescued in both NOX2-deficient macrophages and neutrophils (Figures 7D and 7E).

To determine whether the protection of NOX2-deficient mice against emphysema was directly mediated through SIRT1, we treated elastase-exposed WT and NOX2-deficient mice with sirtinol, a known inhibitor of SIRT1 transcriptional activity [39], or vehicle (Figures 7F–7I). Treatment with sirtinol (2 mg/kg, i.p.) reduced SIRT1 protein levels (Figures 7F and 7G). It also aggravated emphysematous lesions in both elastase-exposed WT and NOX2-deficient mice, as measured by the mean linear intercept (MLI) (Figures 7H

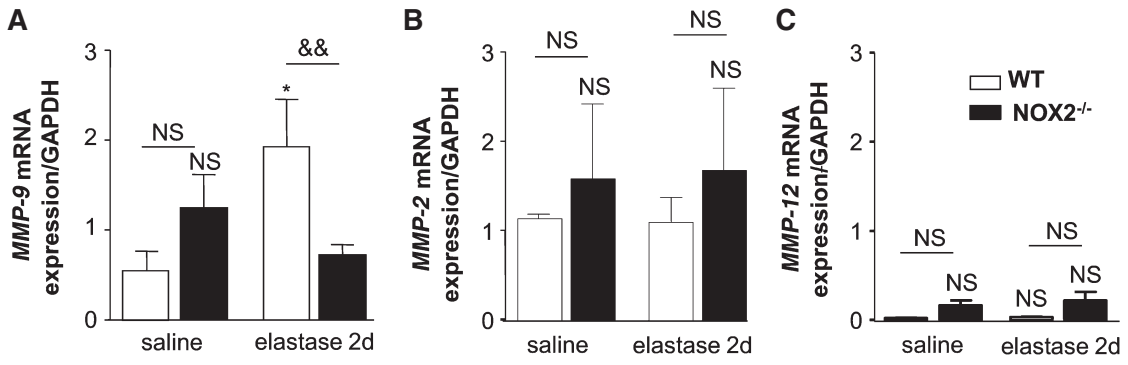

Figure 5. Deficiency of NOX2 reduces elastase-induced *MMP-9* mRNA expression in lungs. Expression of (A) *MMP-9* mRNA, (B) *MMP-2* mRNA, and (C) *MMP-12* mRNA in lung homogenates of WT and NOX2-deficient mice exposed to saline or elastase at day 2 by real-time PCR. Data ± SEM; $n = 3–9$ mice per group; p = NS, $^{*}p < 0.05$ saline versus elastase; $^{\&\&}p < 0.01$ WT versus NOX2$^{-/-}$.

and 7I). It should be noted that the extent of alveolar airspace enlargement observed was significantly lower in NOX2-deficient mice than in WT mice (Figures 7H and 7I).

All of these results indicate that negative regulation of SIRT1 mediated by NOX2 in macrophages and/or neutrophils contributes to elastase-induced emphysema.

Macrophage- but not neutrophil-restricted functional NOX2 contributes to elastase-induced emphysema

As there is some evidence that macrophages rather than neutrophils are involved in emphysema pathogenesis [40,41], we investigated whether NOX2 specifically expressed in monocytes/macrophages caused elastase-induced lung emphysema. For this purpose, we used a mouse model with loss of NOX2 function (*Ncf1* mutant mice) and a mouse line with functional NOX2 rescue (by re-expression of an *Ncf1* gene controlled by the human CD68 promoter on an *Ncf1* mutant B10.Q background; *Ncf1* rescue MN mice) [28]. Importantly, the *Ncf1* mutant mouse differs from its WT control (*Ncf1* WT mice) by only a single mutation and the MN transgene was injected into the *Ncf1* mutant mice; thus, these three strains (*Ncf1* mutant, MN, and WT B10.Q) all share the same genetic background. In addition, the MN mouse has been carefully analysed and expresses Ncf1 only in monocyte/macrophage (including dendritic cells) lineages and not in neutrophils [42].

The production of ROS was measured *in situ* in the three mouse genotypes after saline and elastase instillation, using DHE staining (Figures 8A–8C). Elastase-induced ROS production, which was abolished in *Ncf1* mutant mice, was partially restored in *Ncf1* rescue mice (Figure 8A). We also observed that increased ROS production in macrophages (IBA1-positive cells) and neutrophils (MPO-positive cells) from WT mice following elastase stimulation was completely abolished in *Ncf1* mutant mice. By contrast, ROS production was restored only in macrophages but not in neutrophils from *Ncf1* rescue mice (Figure 8B).

We then evaluated the effect of NOX2-restricted macrophages in elastase-induced alveolar airspace enlargement, as measured by the mean linear intercept (MLI) (Figures 8C and 8D). Elastase stimulation led to increased alveolar airspace enlargement in *Ncf1* WT mice, which was higher in *Ncf1* rescue mice. In *Ncf1* mutant mice, parenchymal destruction was markedly decreased (Figures 8C and 8D). Thus, NOX2-dependent ROS production in macrophages plays a key role in the development of emphysema.

Discussion

In the present study, we found that NOX1 was preferentially expressed in bronchial and alveolar epithelium of emphysematous patients, whereas NOX2 was mainly detected in macrophages, suggesting that NOX1 could play a role in lung alveolar destruction, while NOX2 seems to participate in the inflammatory process in emphysema.

Elastase instillation is an established mouse model of emphysema associated with inflammation [1], protease/anti-protease imbalance [43], and epithelial cell death [44]. We demonstrated that NOX2, but not NOX1 and NOX4, contributed to elastase-induced emphysema, independently in epithelial cell death and in the presence of sustained inflammation. Indeed, NOX2-deficient mice displayed decreased alveolar space enlargement and elastin degradation in lungs compared with WT, NOX1-, and NOX4-deficient mice in response to elastase, without any compensatory regulation of other NOX members. In addition, we found identical indirect cell death parameters (LDH and protein content in BAL; data not shown) and pro-inflammatory profile between all strains. However, we cannot exclude that certain negative results could be due to limited sample size. Nevertheless, an accumulation of apoptotic neutrophils was found in BAL of NOX2-deficient mice at early time points. It has been suggested that impaired efferocytosis of apoptotic neutrophils by NOX2-deficient macrophages [45] as well as modulation of the anti-inflammatory cytokine microenvironment [30,46] may be responsible for this phenotype. Taken together, these results demonstrate

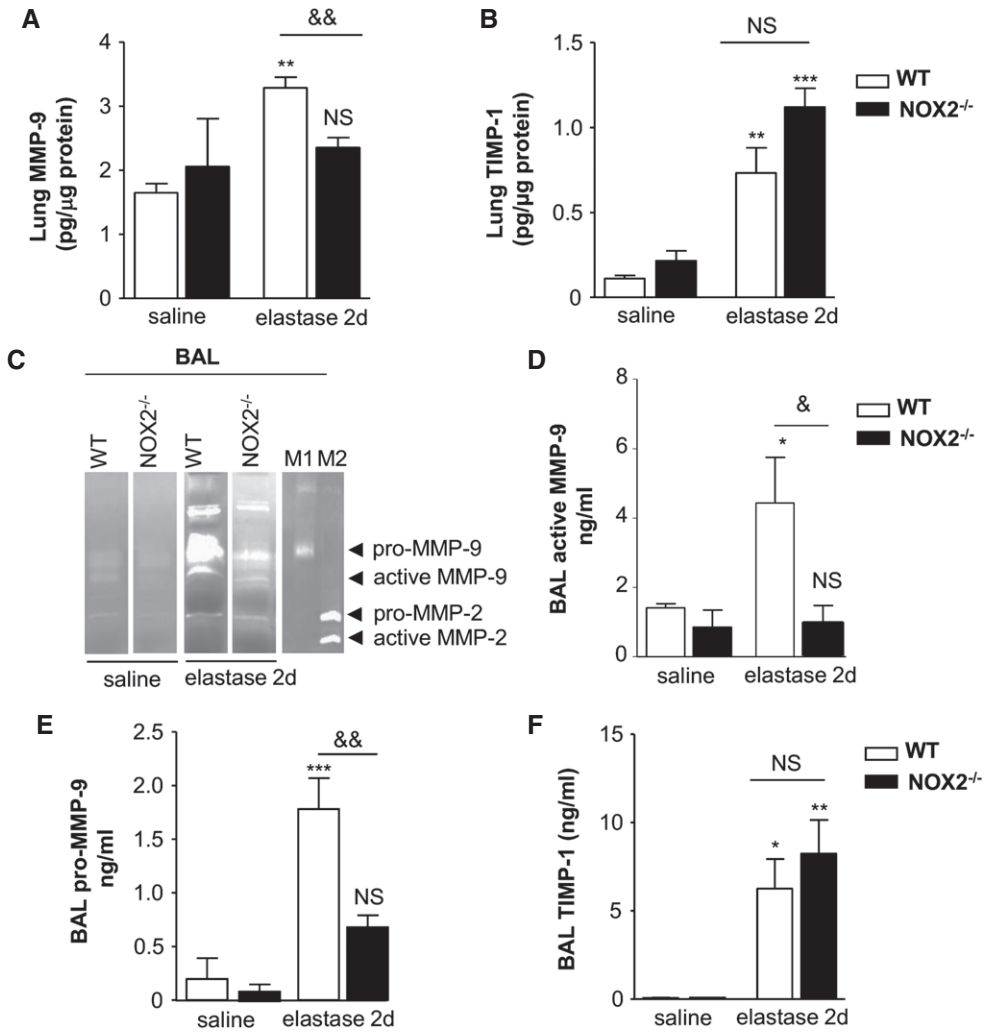

Figure 6. Elastase-induced MMP-9 protein expression and activity are reduced in NOX2-deficient mice. (A) Protein level of MMP-9 was examined in lung homogenates by gelatin zymography and expressed as pg/µg protein. (B) TIMP-1 level was measured in lung homogenates by ELISA and expressed as pg/µg protein. (C) Representative gelatin zymograph of BAL surpernatants. Lane 5 represents control markers for pro- and active MMP-9 (M1) as well as pro- and active MMP-2 (M2). Quantification of active MMP-9 (D), pro-MMP-9 (E), and active + pro-MMP-2 in BAL supernatants expressed as ng/ml of BAL supernatants. (F) TIMP-1 level was measured in BAL supernatants by ELISA and expressed as ng/ml of BAL supernatants. Data ± SEM; $n = 3-7$ mice per group; p = NS, $^{*}p < 0.05$, $^{**}p < 0.01$, $^{***}p < 0.001$ saline versus elastase; $^{\&}p < 0.05$, $^{\&\&}p < 0.01$ WT versus NOX2$^{-/-}$.

that NOX1 and NOX4, preferentially expressed in lung epithelial and endothelial cells, do not contribute to elastase-induced lung cell death associated with emphysema. In contrast, NOX2 in alveolar macrophages and neutrophils is a crucial factor in the development of this disease, despite sustained inflammation.

The contribution of NOX2 to lung inflammation associated with emphysema remains unclear. Indeed, as seen in many other pathological circumstances, NOX2 may have two different roles in emphysema formation, depending on the type of model used: (i) NOX2 may enhance tissue damage through enhanced ROS generation. This patho-mechanism is predominant in the elastase model of emphysema and in smoke-induced emphysema, at early time points [21]; (ii) NOX2 deficiency may enhance tissue damage through hyperinflammation. This mechanism has been suggested for the smoke model of emphysema (ie long-term exposure [23]) and in LPS-induced lung inflammation associated with COPD [21]. Some authors reported spontaneous emphysema formation in NOX2-deficient mice [22,23]. We did not find any emphysematous lesions in aged NOX2-deficient mice bred in specific pathogen-free conditions (Supplementary Figure 5B), but rather observed the classically described interstitial pneumonitis with few granulomas and eosinophilic crystals (Supplementary Figure 5A) [50]. It is possible that spontaneous hyperinflammation and consequently the development of emphysematous lesions could be due to chronic bacterial infections. Indeed, LPS inhalation contributes to the hyperinflammatory response in the CGD mouse model [21] and leads to inflammation-induced emphysema in mice [51].

Concerning the protective effect of NOX2 deficiency in the elastase-induced emphysema model, elastin fragments generated by elastase inhalation seem to play a crucial role in the development of emphysematous lesions [52]. This occurs through the recruitment and

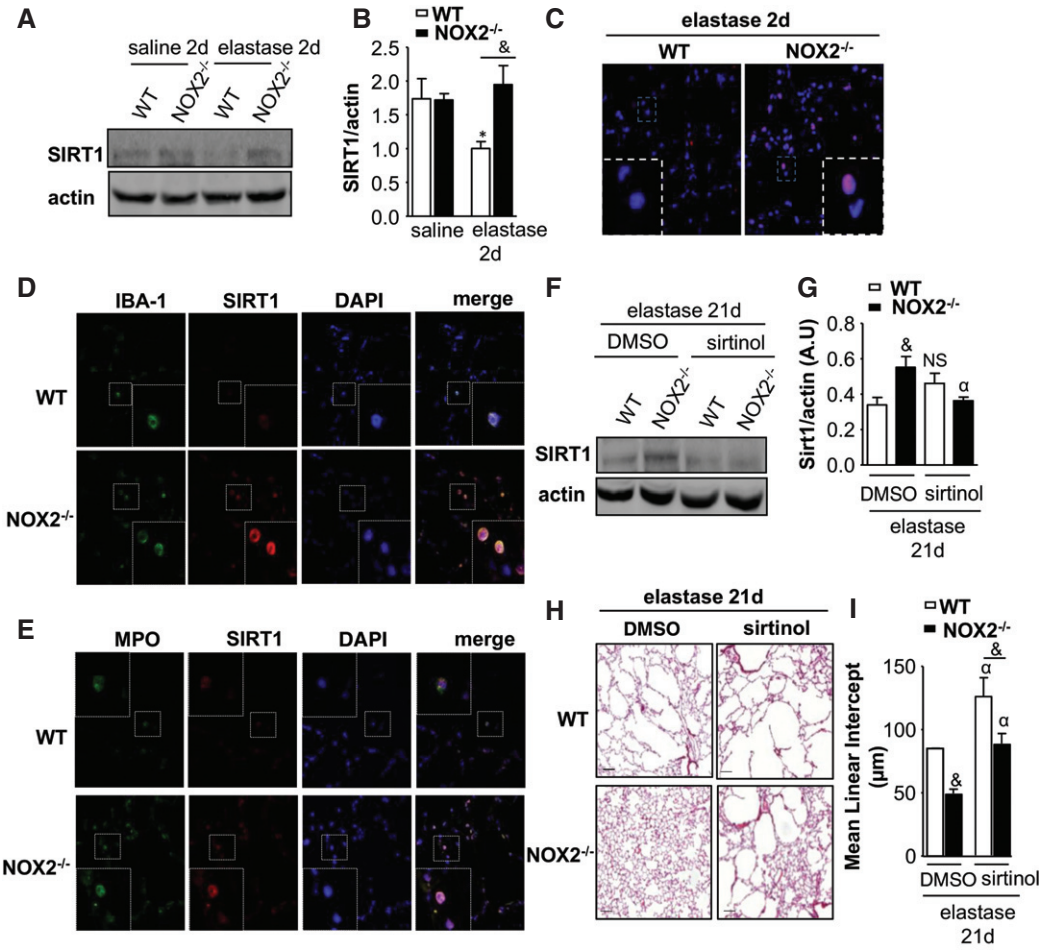

Figure 7. NOX2 contributes to elastase-induced emphysema through negative regulation of SIRT1 in both macrophages and neutrophils. (A) SIRT1 protein was detected in lung homogenates from WT and NOX2-deficient mice exposed to saline or elastase by western blot. β-Actin was used as a loading control. (B) Quantification of SIRT1 protein level in lungs normalized to β-actin ($n = 4$ mice per group). Data ± SEM; $^{*}p < 0.05$ saline versus elastase; $^{\&}p < 0.05$ WT versus NOX2$^{-/-}$. (C) Immunofluorescence of SIRT1 (red) in frozen lung sections. Nuclei are stained with DAPI (blue). SIRT1-positive cells appear in pink. (D, E) Representative images of lung sections stained with SIRT1 (red) and IBA-1 (macrophages, green), or MPO (neutrophils, green). Note that both macrophages and neutrophils are positive for SIRT1 ($n = 3$ mice per group). (F) SIRT1 protein levels of WT and NOX2-deficient mice treated with SIRT1 inhibitor (sirtinol, 2 mg/kg) and exposed to elastase for 21 days were analysed by western blot and (G) quantified by densitometry ($n = 3–4$ mice per group). All samples were normalized with β-actin loading. (H) Lung histology of WT and NOX2-deficient mice treated with sirtinol and exposed to elastase at day 21. Scale bar = 100 µm. (I) Quantification of alveolar diameter expressed as mean linear intercept (L_m, µm). Treatment with sirtinol aggravated emphysematous lesions in both elastase-exposed WT and NOX2-deficient mice ($n = 3–4$ mice per group). Data ± SEM; p = NS; $^{*}p < 0.05$ saline versus elastase; $^{\&}p < 0.05$ WT versus NOX2$^{-/-}$; $^{\alpha}p < 0.05$ DMSO-treated versus sirtinol-treated mice upon elastase exposure.

activation of inflammatory cells, leading to oxidative burst, probably via NOX2 activation, and to the release of MMPs [53] (Figure 9). In this context, the redox modulation of protease/anti-protease balance, in particular the matrix metalloproteinase (MMP)-9/tissue inhibitor of metalloproteinase (TIMP)-1 ratio, is an accepted hypothesis to explain proteolytic destruction associated with elastin fragment-induced emphysema [34,52,54–56]. We demonstrated that NOX2 deficiency decreased elastase-induced mRNA expression and activity of MMP-9, particularly in macrophages and neutrophils, without modification of TIMP-1. Concomitantly, we observed a diminution of elastase-induced ROS production, in particular in macrophages and neutrophils, in the absence of NOX2. Surprisingly, elastase induced ROS generation in epithelial cells, which was inhibited in NOX2-deficient mice. We previously demonstrated that lung epithelial cells do not express NOX2 [10]; it is therefore possible that NOX2-dependent ROS generation by inflammatory cells could contribute to the activation of lung resident cells via paracrine signalling, as demonstrated in other cell types in various pathological conditions [57–59]. Thus, these data suggest that ROS generated by NOX2 activated MMP-9 and modulated its gene expression. Indeed, ROS can directly control MMP-9 activity through interaction with its thiol groups [37]. In parallel, ROS-dependent signalling pathways such as SMAD, cJun, and MAPK [60–62], as well as epigenetic mechanisms related to chromatin acetylation through modulation of histone deacetylase [63], are known to modulate *MMP-9* gene expression. Accordingly, we demonstrated that SIRT1, a histone deacetylase, is negatively regulated by NOX2 in macrophages and

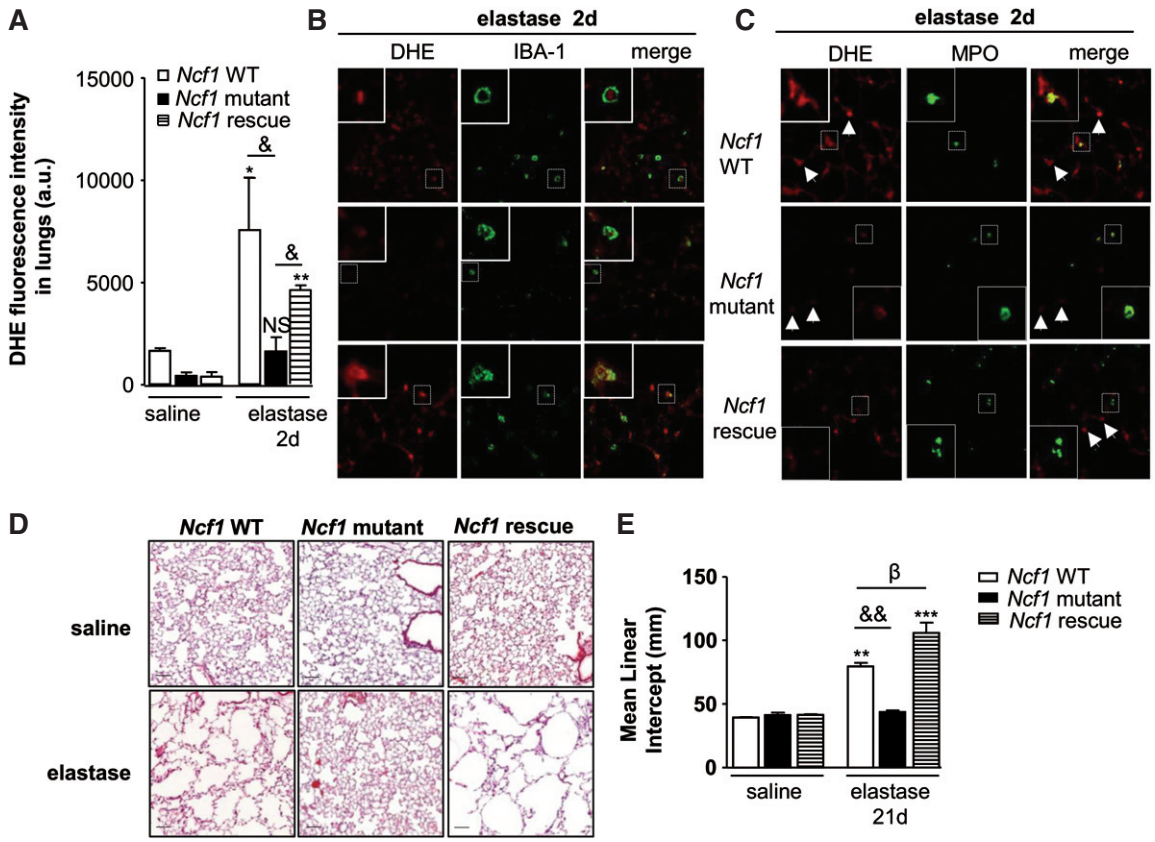

Figure 8. ROS generation by NOX2 specifically in macrophages contributes to the emphysematous phenotype. (A) *Ncf1* WT, *Ncf1* mutant, and *Ncf1* rescue were exposed to elastase or saline and ROS production was analysed at day 2 on frozen lung sections loaded with DHE. DHE fluorescence intensity was quantified for all sections ($n = 3$ mice per group). Data ± SEM; p = NS; $^{*}p < 0.05$, $^{**}p < 0.01$ saline versus elastase; $^{\&}p < 0.05$ *Ncf1* WT versus *Ncf1* mutant, *Ncf1* mutant versus *Ncf1* rescue. Representative images of lung sections stained with DHE (red) and IBA-1 (B) (macrophages, green), or MPO (C) (neutrophils, green). Note that DHE-positive cells were also positive for IBA1 (macrophages) but not for MPO (neutrophils) in *Ncf1* rescue mice following elastase stimulation. Original magnification: ×40. (D) Lung histology of *Ncf1* WT, *Ncf1* mutant, and *Ncf1* rescue exposed to elastase at day 21. Scale bar = 100 µm. (E) Quantification of alveolar diameter expressed as mean linear intercept (L_m, µm). Scale bar = 100 µm ($n = 3$–7 mice per group). Data ± SEM; p = NS; $^{**}p < 0.01$, $^{***}p < 0.001$ saline versus elastase; $^{\&\&}p < 0.01$ *Ncf1* WT versus *Ncf1* mutant; $^{\beta}p < 0.05$ *Ncf1* WT versus *Ncf1* rescue.

neutrophils and is required for the protection afforded by NOX2 deficiency against elastase-induced emphysema. In addition, no difference in SMAD, cJun or MAPK signalling was observed in NOX2-deficient mice. Thus, our results strongly suggest that ROS generated by NOX2 participates in the pathogenesis of emphysema through the modulation of SIRT1/MMP-9 pathways. Our results are supported by previous studies demonstrating that reduced H_2O_2 stimulation as well as PMA, a NOX2 activator, reduced the SIRT1 level in human monocytic cells, probably via proteasome activation leading to its degradation [64,65]. In addition, the decline of the SIRT1 level was associated with elevated MMP-9 expression via an increase in histone acetylation at the activator protein-1- (AP1-), NF-κB-, and Pea3-binding sites of the MMP-9 promoter [38,66]. In contrast, SIRT1 deficiency in epithelial cells, but not in myeloid cells, aggravates cigarette smoke and elastase-induced lung emphysema in mice [29]. These results are not incompatible with our data for two reasons. First, the FOXO3/p21 pathway mediates SIRT1 protection against emphysema in epithelial cells independently of MMP-9. Second, MMP-9 expression negatively mediated by SIRT1 in myeloid cells is necessary but not sufficient to lead to proteolytic damage; indeed, its activation is required. Thus, negative regulation of *MMP-9* gene expression through SIRT1, and decreased MMP-9 activity in macrophages and neutrophils are important mechanisms to explain the protection afforded to NOX2-deficient mice against emphysema.

Finally, although we have shown that NOX2 in macrophages and neutrophils plays a role in the pathogenesis of emphysema, the contribution of macrophages/monocytes versus neutrophils in this context has until now been unclear. To dissociate their roles, we used the elastase-induced emphysema model in three different mouse constructs: *Ncf1* mutant mice carrying natural *Ncf1* mutation and presenting non-functional NOX2; *Ncf1* rescue mice with functional NOX2 only in CD68-positive monocytes/macrophages; and *Ncf1* control WT mice [28]. We clearly showed that functional NOX2 expressed only in macrophages/monocytes is sufficient to induce emphysema. This is supported by studies demonstrating that depletion of macrophages,

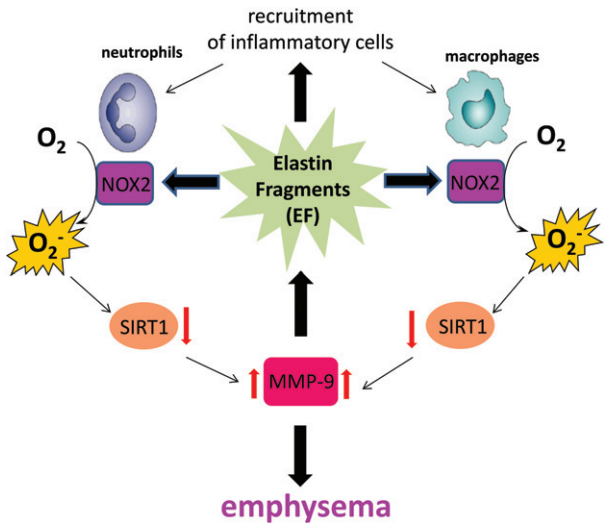

Figure 9. Schematic representation of the role of NOX2 in elastase-induced emphysema. At early time points, elastin fragments (EF) produced by elastase inhalation drive the recruitment and activation of both macrophages and neutrophils. EF lead to NOX2-dependent ROS generation that controls MMP-9 activity and gene expression through negative regulation of SIRT-1. This leads to extracellular matrix proteolysis with production of new EF and development of emphysema. These new fragments in turn control NOX2 activation and NOX2-dependent SIRT1/MMP-9 pathways. At later time points, when neutrophils are cleared, lung macrophages mainly contribute to pathology progression.

but not neutrophils, contributes to CS-induced emphysema [40,41]. In addition, these results confirm our previous data from NOX2-deficient mice and show that the effect of NOX2 in the pathogenesis of emphysema is not dependent on 129 linked genes carried over from the embryonic stem cells, the knockout construct or on the C57Bl/6 background, since the results could be repeated using *Ncf1*-mutated mice on a genetically controlled B10.Q background.

In summary, NOX2 is expressed in lung macrophages in emphysematous patients and contributes to elastase-induced emphysema through the modulation of SIRT1/MMP-9 pathways. In addition, the rescue of functional NOX2 specifically in macrophages contributes to the development of emphysema. A better understanding of NOX isoforms in different emphysema-relevant cell types should provide the opportunity to define new therapeutic strategies in the management of emphysema.

Acknowledgments

This study was supported by the Swiss National Foundation, Marie-Heim Vögltin (SC), Ligue Pulmonaire Suisse (SC), and Ligue Pulmonaire Genevoise (SC), and also by the European Community Framework Programme under grant agreements NEURINOX (Health-F2-2011-278611) and the KA Wallenberg Foundation (RH). We would like to thank S Startchik, O Plastre, T Cagarelli, L Beer, Y Hourier, and P Henchoz for technical assistance and help, and JD Lambeth for the anti-NOX1 antibody.

Author contribution statement

CT, CD, JC, YD, CT, SP, VB, J-CP, KHK, RH, CB-A, and SC conceived experiments. CT, CD, JC, YD, CT, SP, VB, and J-CP carried out and analysed data. All authors were involved in writing the paper and had final approval of the submitted and published versions.

Abbreviations

BAL, bronchoalveolar lavage; CGD, chronic granulomatous disease; MPO, myeloperoxidase; Ncf1, neutrophil cytosolic factor; NOX, nicotinamide adenine dinucleotide phosphate oxidase; PAF, paraformaldehyde; SP-C, pro-surfactant C; SPF, specific pathogen-free; TIMP, tissue inhibitors of metalloproteinases

References

1. Taraseviciene-Stewart L, Voelkel NF. Molecular pathogenesis of emphysema. *J Clin Invest* 2008; **118:** 394–402.
2. Montuschi P, Collins JV, Ciabattoni G, *et al.* Exhaled 8-isoprostane as an *in vivo* biomarker of lung oxidative stress in patients with COPD and healthy smokers. *Am J Respir Critical Care Med* 2000; **162:** 1175–1177.
3. Nowak D, Kasielski M, Antczak A, *et al.* Increased content of thiobarbituric acid-reactive substances and hydrogen peroxide in the expired breath condensate of patients with stable chronic obstructive pulmonary disease: no significant effect of cigarette smoking. *Respir Med* 1999; **93:** 389–396.
4. Praticò D, Basili S, Vieri M, *et al.* Chronic obstructive pulmonary disease is associated with an increase in urinary levels of isoprostane F2alpha-III, an index of oxidant stress. *Am J Respir Crit Care Med* 1998; **158:** 1709–1714.
5. Rahman I, Bel A, Mulier B, *et al.* Differential regulation of glutathione by oxidants and dexamethasone in alveolar epithelial cells. *Am J Physiol* 1998; **275:** L80-L86.
6. Kirkham PA, Barnes PJ. Oxidative stress in COPD. *Chest* 2013; **144:** 266–273.
7. Lambeth JD. NOX enzymes and the biology of reactive oxygen. *Nature Rev Immunol* 2004; **4:** 181–189.
8. Bedard K, Krause KH. The NOX family of ROS-generating NADPH oxidases: physiology and pathophysiology. *Physiol Rev* 2007; **87:** 245–313.
9. Babior BM. The leukocyte NADPH oxidase. *Isr Med Assoc J* 2002; **4:** 1023–1024.
10. Carnesecchi S, Deffert C, Pagano A, *et al.* NADPH oxidase-1 plays a crucial role in hyperoxia-induced acute lung injury in mice. *Am J Respir Crit Care Med* 2009; **180:** 972–981.
11. Miyoshi T, Yamashita K, Arai T, *et al.* The role of endothelial interleukin-8/NADPH oxidase 1 axis in sepsis. *Immunology* 2010; **131:** 331–339.
12. Carnesecchi S, Deffert C, Donati Y, *et al.* A key role for NOX4 in epithelial cell death during development of lung fibrosis. *Antioxid Redox Signal* 2011; **15:** 607–619.
13. Hecker L, Vittal R, Jones T, *et al.* NADPH oxidase-4 mediates myofibroblast activation and fibrogenic responses to lung injury. *Nature Med* 2009; **15:** 1077–1081.

14. Pache JC, Carnesecchi S, Deffert C, *et al.* NOX-4 is expressed in thickened pulmonary arteries in idiopathic pulmonary fibrosis. *Nature Med* 2011; **17:** 31–32; author reply 32–33.
15. Park HS, Chun JN, Jung HY, *et al.* Role of NADPH oxidase 4 in lipopolysaccharide-induced proinflammatory responses by human aortic endothelial cells. *Cardiovasc Res* 2006; **72:** 447–455.
16. Park HS, Jung HY, Park EY, *et al.* Cutting edge: direct interaction of TLR4 with NAD(P)H oxidase 4 isozyme is essential for lipopolysaccharide-induced production of reactive oxygen species and activation of NF-kappa B. *J Immunol* 2004; **173:** 3589–3593.
17. Pongnimitprasert N, Hurtado M, Lamari F, *et al.* Implication of NADPH oxidases in the early inflammation process generated by cystic fibrosis cells. *ISRN Inflamm* 2012; **2012:** 481432.
18. Sutcliffe A, Hollins F, Gomez E, *et al.* Increased nicotinamide adenine dinucleotide phosphate oxidase 4 expression mediates intrinsic airway smooth muscle hypercontractility in asthma. *Am J Respir Crit Care Med* 2012; **185:** 267–274.
19. Kim SY, Moon KA, Jo HY, *et al.* Anti-inflammatory effects of apocynin, an inhibitor of NADPH oxidase, in airway inflammation. *Immunol Cell Biol* 2012; **90:** 441–448.
20. Meng QR, Gideon KM, Harbo SJ, *et al.* Gene expression profiling in lung tissues from mice exposed to cigarette smoke, lipopolysaccharide, or smoke plus lipopolysaccharide by inhalation. *Inhal Toxicol* 2006; **18:** 555–568.
21. Lagente V, Planquois JM, Leclerc O, *et al.* Oxidative stress is an important component of airway inflammation in mice exposed to cigarette smoke or lipopolysaccharide. *Clin Exp Pharmacol Physiol* 2008; **35:** 601–605.
22. Zhang X, Shan P, Jiang G, *et al.* Toll-like receptor 4 deficiency causes pulmonary emphysema. *J Clin Invest* 2006; **116:** 3050–3059.
23. Yao H, Edirisinghe I, Yang SR, *et al.* Genetic ablation of NADPH oxidase enhances susceptibility to cigarette smoke-induced lung inflammation and emphysema in mice. *Am J Pathol* 2008; **172:** 1222–1237.
24. Gianni D, Bohl B, Courtneidge SA, *et al.* The involvement of the tyrosine kinase c-Src in the regulation of reactive oxygen species generation mediated by NADPH oxidase-1. *Mol Biol Cell* 2008; **19:** 2984–2994.
25. Antony S, Wu Y, Hewitt SM, *et al.* Characterization of NADPH oxidase 5 expression in human tumors and tumor cell lines with a novel mouse monoclonal antibody. *Free Radic Biol Med* 2013; **65:** 497–508.
26. Gavazzi G, Banfi B, Deffert C, *et al.* Decreased blood pressure in NOX1-deficient mice. *FEBS Lett* 2006; **580:** 497–504.
27. Pollock JD, Williams DA, Gifford MA, *et al.* Mouse model of X-linked chronic granulomatous disease, an inherited defect in phagocyte superoxide production. *Nature Genet* 1995; **9:** 202–209.
28. Gelderman KA, Hultqvist M, Pizzolla A, *et al.* Macrophages suppress T cell responses and arthritis development in mice by producing reactive oxygen species. *J Clin Invest* 2007; **117:** 3020–3028.
29. Yao H, Chung S, Hwang JW, *et al.* SIRT1 protects against emphysema via FOXO3-mediated reduction of premature senescence in mice. *J Clin Invest* 2012; **122:** 2032–2045.
30. Deffert C, Carnesecchi S, Yuan H, *et al.* Hyperinflammation of chronic granulomatous disease is abolished by NOX2 reconstitution in macrophages and dendritic cells. *J Pathol* 2012; **228:** 341–350.
31. Deryugina EI, Zijlstra A, Partridge JJ, *et al.* Unexpected effect of matrix metalloproteinase down-regulation on vascular intravasation and metastasis of human fibrosarcoma cells selected *in vivo* for high rates of dissemination. *Cancer Res* 2005; **65:** 10959–10969.
32. Trocme C, Gaudin P, Berthier S, *et al.* Human B lymphocytes synthesize the 92-kDa gelatinase, matrix metalloproteinase-9. *J Biol Chem* 1998; **273:** 20677–20684.
33. Carnesecchi S, Dunand-Sauthier I, Zanetti F, *et al.* NOX1 is responsible for cell death through STAT3 activation in hyperoxia and is associated with the pathogenesis of acute respiratory distress syndrome. *Int J Clin Exp Pathol* 2014; **7:** 537–551.
34. Foronjy R, Nkyimbeng T, Wallace A, *et al.* Transgenic expression of matrix metalloproteinase-9 causes adult-onset emphysema in mice associated with the loss of alveolar elastin. *Am J Physiol Lung Cell Mol Physiol* 2008; **294:** L1149-L1157.
35. Wallace AM, Sandford AJ, English JC, *et al.* Matrix metalloproteinase expression by human alveolar macrophages in relation to emphysema. *COPD* 2008; **5:** 13–23.
36. Sundar IK, Yao H, Rahman I. Oxidative stress and chromatin remodeling in chronic obstructive pulmonary disease and smoking-related diseases. *Antioxid Redox Signal* 2013; **18:** 1956–1971.
37. Nelson KK, Melendez JA. Mitochondrial redox control of matrix metalloproteinases. *Free Radic Biol Med* 2004; **37:** 768–784.
38. Nakamaru Y, Vuppusetty C, Wada H, *et al.* A protein deacetylase SIRT1 is a negative regulator of metalloproteinase-9. *FASEB J* 2009; **23:** 2810–2819.
39. Grozinger CM, Chao ED, Blackwell HE, *et al.* Identification of a class of small molecule inhibitors of the sirtuin family of NAD-dependent deacetylases by phenotypic screening. *J Biol Chem* 2001; **276:** 38837–38843.
40. Hautamaki RD, Kobayashi DK, Senior RM, *et al.* Requirement for macrophage elastase for cigarette smoke-induced emphysema in mice. *Science* 1997; **277:** 2002–2004.
41. Ofulue AF, Ko M. Effects of depletion of neutrophils or macrophages on development of cigarette smoke-induced emphysema. *Am J Physiol* 1999; **277:** L97-L105.
42. Pizzolla A, Hultqvist M, Nilson B, *et al.* Reactive oxygen species produced by the NADPH oxidase 2 complex in monocytes protect mice from bacterial infections. *J Immunol* 2012; **188:** 5003–5011.
43. Wright JL, Cosio M, Churg A. Animal models of chronic obstructive pulmonary disease. *Am J Physiol Lung Cell Mol Physiol* 2008; **295:** L1-L15.
44. Hou HH, Cheng SL, Liu HT, *et al.* Elastase induced lung epithelial cell apoptosis and emphysema through placenta growth factor. *Cell Death Dis* 2013; **4:** e793.
45. Fernandez-Boyanapalli RF, Frasch SC, McPhillips K, *et al.* Impaired apoptotic cell clearance in CGD due to altered macrophage programming is reversed by phosphatidylserine-dependent production of IL-4. *Blood* 2009; **113:** 2047–2055.
46. Zeng MY, Pham D, Bagaitkar J, *et al.* An efferocytosis-induced, IL-4-dependent macrophage-iNKT cell circuit suppresses sterile inflammation and is defective in murine CGD. *Blood* 2013; **121:** 3473–3483.
47. Mahdaviani SA, Mohajerani SA, Rezaei N, *et al.* Pulmonary manifestations of chronic granulomatous disease. *Expert Rev Clin Immunol* 2013; **9:** 153–160.
48. Mahdaviani SA, Mehrian P, Najafi A, *et al.* Pulmonary computed tomography scan findings in chronic granulomatous disease. *Allergol Immunopathol (Madr)* 2013; DOI:10.1016/j.aller.2013.04.003.
49. van den Berg JM, van Koppen E, Ahlin A, *et al.* Chronic granulomatous disease: the European experience. *PLoS One* 2009; **4:** e5234.
50. Liu Q, Cheng LI, Yi L, *et al.* p47phox deficiency induces macrophage dysfunction resulting in progressive crystalline macrophage pneumonia. *Am J Pathol* 2009; **174:** 153–163.
51. Vernooy JH, Dentener MA, van Suylen RJ, *et al.* Long-term intratracheal lipopolysaccharide exposure in mice results in chronic lung inflammation and persistent pathology. *Am J Respir Cell Mol Biol* 2002; **26:** 152–159.

52. Houghton AM, Quintero PA, Perkins DL, *et al.* Elastin fragments drive disease progression in a murine model of emphysema. *J Clin Invest* 2006; **116:** 753–759.
53. Adair-Kirk TL, Senior RM. Fragments of extracellular matrix as mediators of inflammation. *Int J Biochem Cell Biol* 2008; **40:** 1101–1110.
54. Barnes PJ. Mediators of chronic obstructive pulmonary disease. *Pharmacol Rev* 2004; **56:** 515–548.
55. Gosselink JV, Hayashi S, Elliott WM, *et al.* Differential expression of tissue repair genes in the pathogenesis of chronic obstructive pulmonary disease. *Am J Respir Crit Care Med* 2010; **181:** 1329–1335.
56. Culpitt SV, Rogers DF, Traves SL, *et al.* Sputum matrix metalloproteases: comparison between chronic obstructive pulmonary disease and asthma. *Respir Med* 2005; **99:** 703–710.
57. Li WG, Miller FJ Jr, Zhang HJ, *et al.* H(2)O(2)-induced O(2) production by a non-phagocytic NAD(P)H oxidase causes oxidant injury. *J Biol Chem* 2001; **276:** 29251–29256.
58. Haurani MJ, Pagano PJ. Adventitial fibroblast reactive oxygen species as autacrine and paracrine mediators of remodeling: bellwether for vascular disease? *Cardiovasc Res* 2007; **75:** 679–689.
59. Waghray M, Cui Z, Horowitz JC, *et al.* Hydrogen peroxide is a diffusible paracrine signal for the induction of epithelial cell death by activated myofibroblasts. *FASEB J* 2005; **19:** 854–856.
60. Rhee JW, Lee KW, Sohn WJ, *et al.* Regulation of matrix metalloproteinase-9 gene expression and cell migration by NF-kappa B in response to CpG-oligodeoxynucleotides in RAW 264.7 cells. *Mol Immunol* 2007; **44:** 1393–1400.
61. Spallarossa P, Altieri P, Garibaldi S, *et al.* Matrix metalloproteinase-2 and −9 are induced differently by doxorubicin in H9c2 cells: the role of MAP kinases and NAD(P)H oxidase. *Cardiovasc Res* 2006; **69:** 736–745.
62. Xu B, Chen H, Xu W, *et al.* Molecular mechanisms of MMP9 overexpression and its role in emphysema pathogenesis of Smad3-deficient mice. *Am J Physiol Lung Cell Mol Physiol* 2012; **303:** L89-L96.
63. Labrie M, St-Pierre Y. Epigenetic regulation of *mmp-9* gene expression. *Cell Mol Life Sci* 2013; **70:** 3109–3124.
64. Salminen A, Kaarniranta K, Kauppinen A. Crosstalk between oxidative stress and SIRT1: impact on the aging process. *Int J Mol Sci* 2013; **14:** 3834–3859.
65. Caito S, Rajendrasozhan S, Cook S, *et al.* SIRT1 is a redox-sensitive deacetylase that is post-translationally modified by oxidants and carbonyl stress. *FASEB J* 2010; **24:** 3145–3159.
66. Padilla ML, Galicki NI, Kleinerman J, *et al.* High cathepsin B activity in alveolar macrophages occurs with elastase-induced emphysema but not with bleomycin-induced pulmonary fibrosis in hamsters. *Am J Pathol* 1988; **131:** 92–101.

SUPPORTING INFORMATION ON THE INTERNET

The following supporting information may be found in the online version of this article:

Supplementary materials and methods.

Figure S1. NOX2 deficiency does not modulate NOX members' mRNA expression after elastase treatment.

Figure S2. Pro-inflammatory cytokines and chemokines are not modulated in NOX2-deficient mice after elastase treatment.

Figure S3. MMP-2 protein level is not modified in NOX2-deficient mice exposed to elastase.

Figure S4. NOX2 deficiency prevents decreased SIRT1 associated with elastase instillation.

Figure S5. NOX2-deficient mice at 12 months of age do not develop spontaneous emphysema, but display interstitial pneumonitis with eosinophilic crystals and few granulomas.